JOURNAL OF Applied Polymer SCIENCE

Morphological Properties of Impact Fracture Surfaces and Essential Work of Fracture Analysis of Cellulose Nanofibril-Filled Polypropylene Composites

Han-Seung Yang, Douglas J. Gardner, Jacques W. Nader
AEWC-Advanced Structures and Composites Center, University of Maine, Orono, Maine 04469-5793
Correspondence to: H.-S. Yang (E-mail: hsyang@umn.edu) and D. J. Gardner (E-mail: douglasg@maine.edu)

ABSTRACT: Scanning electron microscopy (SEM) was employed to investigate crack initiation and propagation process in notched and unnotched Izod impact fracture surfaces of the cellulose nanofiber (CNF) and microfibrillated cellulose (MFC)-filled polypropylene (PP) composites compared with microcrystalline cellulose (MCC)-filled composites. CNF is in the form of short fibers 50–300 nm in diameter and 6–8 in aspect ratio, MFC is in the form of long fibrils 50–500 nm in diameter and 8,000–80,000 in aspect ratio, and MCC is in the form of particles 50 μm in average diameter and 1–2 in aspect ratio. The reinforcement material size of CNF and MFC are smaller than that of MCC which means that the larger interfacial area between filler and matrix leading to larger energy dissipation at the interface during the impact fracture. The reinforcement-matrix debondings nearby MCC particles caused easy crack propagation which contributes smaller energy dissipation at the interface. A slip-stick behavior and stress whitened area during the fracture were observed. Morphological investigation helps to explain impact fracture behavior. According to essential work of fracture (EWF) analysis of Izod impact results, EWF method is applicable to analyze impact fracture behavior and the energy consumed in crack initiation and propagation during the fracture process can be calculated. © 2012 Wiley Periodicals, Inc. J. Appl. Polym. Sci. 000: 000–000, 2012

Received 15 February 2012; accepted 22 August 2012; published online
DOI: 10.1002/app.38513

INTRODUCTION

Cellulose is an abundant organic resource used as a natural reinforcement material to reinforce composites; its overall properties are comparable with other inorganic reinforcements. It has been found that cellulose-reinforced composites have desirable mechanical properties.[1] In addition, the low cost of cellulose relative to inorganic materials, its relative high-strength, high stiffness and low density are positive properties. Therefore, natural reinforcement material can be a replacement for synthetic reinforcements to reinforce plastics used in the automotive industry, packaging, and furniture production.[2] Considerable effort has been devoted in recent years to the research and development of materials that utilize cellulose fibers as the load bearing constituents for various polymeric composites.[3] Since cellulose represents the primary structural component of plants[4] and has positive attributes such as renewability and biodegradability, there are major incentives for exploring new uses.[5] Cellulose nanofibrils are emerging as an important new application of cellulose in reinforcing materials. Generally, cellulose nanofibers (CNF) are the elementary assemblies of distinct polymeric units based on glucopyranose that can have diameters on the order of tens of nanometers and constitute a fiber of the strand. Their unique structural aspects give them unique tensile, optical, electrical, and chemical properties unlike their macroscopic counterparts such as microfibers or larger structures.[6] The term "fibril" has been used by various researchers to describe relatively long and very thin pieces of cellulosic material.[3,7–11] Meanwhile, the term "nanofibers" has come into increasing use, which helps to emphasize cases where very small cellulosic fibrous materials can display behavior and functionality that differ from what has been observed with larger cellulosic fibers.[6]

Polyolefins are relatively low cost polymers and when reinforced with low cost lignocellulosic fillers, properties can be achieved which correspond to more expensive engineering polymers.[12] Polypropylene (PP) is suitable as a matrix polymer because of its low price and favorable properties such as stiffness, light weight, weathering ability, design flexibility, and mechanical properties.[1] To improve the competitiveness of PP for engineering plastic applications, it is an important objective in PP compounding to simultaneously increase its dimensional stability, heat distortion temperature, stiffness, strength, and impact resistance without sacrificing easy processing.[13] Certain composite applications need high modulus and brittleness, but others need good stiffness and ductility. Fracture toughness and impact

resistance are among the most important mechanical properties of a material when impact loading is applied. Determination of fracture characteristics, therefore, is extremely important.[14] Especially for applications in motor vehicle exteriors such as bumpers and impact-resistant panels, fracture initiation, and propagation mechanisms are a key factor of a material's property requirements. There are few reported investigations dealing with analyses of the individual stages of the fracture process under impact loading applications.[14–17]

The significant increase in modulus of elasticity of cellulose nanofibril-reinforced thermoplastic polymer composites is recognized and is reasonably understood. However, an understanding of the toughness behavior is still fragmented and less examined. It is important to examine impact toughness considering that the majority of semicrystalline polymeric materials such as PP are ductile at low strain rates, but at high strain rates such as those experienced in an Izod impact test, these materials exhibit brittle behavior. Thus, the study of impact toughness at higher strain rates is of particular interest and relevant because yield stress increases with strain rate, promoting a brittle mode of fracture.[18]

In an impact strength analysis study[19], the impact properties of CNF and microfibrillated cellulose (MFC)-filled PP composites were evaluated and compared with microcrystalline cellulose (MCC)-filled composites including discussion of individual impact energy behavior during fracture. The impact resistance of the material was analyzed by newly developed "characteristic impact resistance model" as additional analysis technique compared with conventional impact property analysis. CNF was the most excellent material among the others in terms of both impact resistance and characteristic impact resistance because the size of CNF is smallest and the shape is short rod-like form leading to a largest interfacial area. MFC-filled composites exhibit lower impact resistance than MCC-filled composites in terms of conventional impact resistance but MFC is better in terms of characteristic impact resistance. Scanning electron microscopy (SEM) was used in this study for structure determination of the composites using various natural fillers as reinforcements.[20] In all studies, fracture surfaces of cellulose nanofibril-filled PP composite samples were generated and coated to avoid charging.

The essential work of fracture (EWF) theory has already been used widely to analyze the fracture behavior of composite materials[21–29] and it is also useful to investigate fracture initiation and the propagation process of composite materials. The toughness of the materials is generally characterized by standard impact tests, such as notched and unnotched Izod or Charpy impact tests but the fracture energies obtained by these tests are depend on sample dimensions, crack geometry, and rate of deformation etc. The differences and similarities between Izod impact and DDENT (deeply double edge-notched tension) test will be discussed because this study applied EWF method to analyze Izod impact behavior of the material.

In this study, SEM was employed for the morphological characterization of the impact fracture surfaces. Also, the EWF analysis was adapted to the Izod impact test results by means of notched impact test results. From the EWF analysis, the amount of energy consumed to initiate as well as propagate fracture can be calculated. The purpose of morphological study is to help describe the impact fracture mechanism of composites using SEM micrographs.

EXPERIMENTAL

Materials

Matrix Polymer. The PP used as the thermoplastic matrix polymer was supplied by Polystrand Co. (Montrose, CO), in the form of impact modified copolymer pellets with a density of 900 kg/m^3 and a melt flow index of 35 g/10 min (230°C/2160 g). Its commercial product name is FHR Polypropylene AP5135-HS; it was stored in sealed packages.

Reinforcements. The cellulose materials used as natural reinforcements in the composites were MCC for comparison purposes, CNF and MFC. The product name of the MCC was Sigmacell® Cellulose Type 50 supplied by Sigma-Aldrich Co. (St. Louis, MO), CNF was Arbocel Nano MF 40-10 supplied by J. Rettenmaier & Söhne GMBH Co. (Rosenberg, Germany) and the MFC was Lyocell L010-4 supplied by EFTec™ Co. (Shelton, CT). CNF was in the form of a suspension with a solids content of 10 wt %. MFC was in the form of a wet fiber web with a solids content of 15 wt %. CNF is in the form of rod-like short fibers 50–300 nm in diameter and 6–8 in aspect ratio, MFC is in the form of long fibrils 50–500 nm in diameter and 8,000–80,000 in aspect ratio, and MCC is in the form of particles 50 μm in average diameter and 1–2 in aspect ratio. The MCC was stored in sealed containers after being oven-dried for 24 h at 103°C. The CNF and MFC were stored in a refrigerator at 5–10°C in sealed packages before being used.

Sample Preparation

The MCC was dried to a moisture content of less than 1 wt % using a forced air oven at 103°C for at least 24 h and then stored in sealed containers in an environmental chamber before compounding. The CNF and MFC were stored in sealed containers in a refrigerator before compounding. A Brabender (Duisburg, Germany) Prep-mixer® was used to compound the MCC, CNF, and MFC with the PP, with the latter being used as a matrix polymer. During the CNF and MFC mixing with PP, the cellulose nanofibril suspension and wet fiber webs were slowly and carefully fed into the bowl mixer in very low amounts such as couple of milligrams for each attempt, otherwise the water would evaporate explosively and violently. This procedure took 8 min. The MCC powder was slowly fed into the bowl mixer for 2 min. The process temperature and torque changes were measured in real time. The sample preparation procedure consisted of three general processes, viz. melt blending, grinding, and injection molding. Compounding was performed at 190°C for 40 min including cellulose reinforcement feeding time with a screw speed of 60 rpm. After being oven-dried for at least 24 h at 103°C, the blended mixture was granulated using a laboratory scale grinder; the ground particles were stored in sealed packs to avoid unexpected moisture infiltration. Five levels of reinforcement loading (1, 2, 3, 4, and 8 wt %) for MCC, CNF, and MFC were used in the Izod impact strength measurement and composites containing 3 wt % of

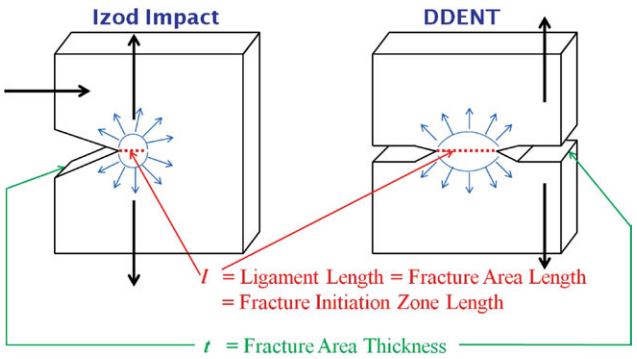

Figure 1. Schematic comparison of Izod impact and DDENT test samples. [Color figure can be viewed in the online issue, which is available at wileyonlinelibrary.com.]

reinforcement were chosen to investigate SEM micrographs. Ground particles were stored in sealed containers in an environmental chamber prior to injection molding. The samples used for the Izod impact tests were injection molded at 246°C, using an injection pressure of 17.25 MPa. Since the mixture was kept just 10 sec in the injection molding machine, such a high temperature is needed to be melted effectively and there was no evidence of thermal decomposition. The width, length, and depth of the impact test samples were in accordance with ASTM D 256-06. The impact sample was directly obtained by injection molding because there is custom made mold exactly fits the sample size in ASTM D 256-06. After injection molding, the test samples were conditioned before testing at 23 ± 2°C and 50 ± 5% RH for at least 40 h according to ASTM D 618-99.

Test Methods

Izod Impact Tests. Notched and unnotched Izod impact strength tests were conducted using a Ceast pendulum impact tester (Model Resil 50B) according to ASTM D 256-06 at 23 ± 2°C and 50 ± 5% RH in the environmentally conditioned mechanical testing room. Each value obtained represented the average of six samples and in the case where COV (coefficient of variance) exceeded 5%, the number of samples was increased to 20.

Scanning Electron Microscopy (SEM). Studies on the morphology of the Izod impact fracture surfaces of the composites were carried out using an AMR 1000 (AMRay Co., Bedford, MA) scanning electron microscope (SEM). Images were taken at 10 kV with 20×, 2000×, and 12000× SEM micrograph magnifications. All samples were sputtered with gold before the microscopic observations were obtained.

Essential Work of Fracture (EWF) Theory

The EWF theory has been widely used to analyze composite materials' fracture behavior and fracture resistance since the first EWF protocol[30] and it is useful to investigate the fracture initiation and propagation process of composite materials. In this study, the EWF concept was adapted to the Izod impact test results by using impact resistance and fracture initiated zone length. Basically the DDENT (deeply double edge-notched tension) test is based on tensile load with controlled fracture initiation zone length which is ligament length. But in the case of Izod impact test, the fracture initiation zone length cannot be controlled but only can be measured after fracture occurred, therefore ligament length (l) in EWF theory replaces fracture initiation zone length in this study but both the Izod impact fracture and DDENT fracture are involved in the stress whitened area which is the fracture initiation zone as indicated and compared in Figure 1. Most works dealing with the EWF concept were done at quasi-static loading conditions which are mainly applied to the highly ductile materials, films, and thin plates. On the other hand, a relatively small number of papers at impact loading conditions using mostly thicker samples have been published in recent years.[31–41] The fracture energy data revealed from standard Izod or Charpy impact tests are sum of the any kind of energy which can be absorbed during test. In some cases, EWF concept can be utilized as an effective method for the determination of fracture toughness of ductile polymers having sharp cracks deformed at high rates.[33] Once the EWF concept was extended to impact loading conditions, great attention was paid to this method due to its simplicity and useful information that was drawn out to understand fracture behavior of polymers, polymer blends, and composites under high rate of deformations.[33] However, it has sometimes led to a non-critical use of EWF concept with respect to methodical preconditions and requirements for the sample geometry.[42] Unaffected by the speed of loading or the shape and dimension of the samples, the most important preconditions for applying EWF concept are (i) initiation of stable crack growth must occur after the yielding of the full ligament, (ii) stable crack propagation, and (iii) self-similarity of all load-displacement diagrams.[42] The method of previous researchers[43] is somewhat similar to the EWF method but was developed for semi-ductile materials at which both stable and unstable crack propagation have been observed. Visual inspection of the sample during the experiments indicated that crack propagated before the completion of the fully yielding of the ligament in this study and this means that criterion was not satisfied. However, even in the presence of dissatisfaction in yielding criterion of EWF, previous researchers demonstrated applicability of EWF methodology using a different notation.[44] In this study, the fracture area is not the total cross section of the sample but limited to crack

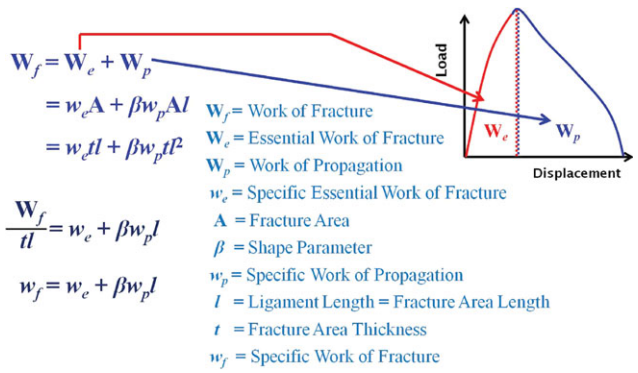

Figure 2. Typical load-displacement curve of DDENT test in EWF concept. [Color figure can be viewed in the online issue, which is available at wileyonlinelibrary.com.]

Applied Polymer SCIENCE

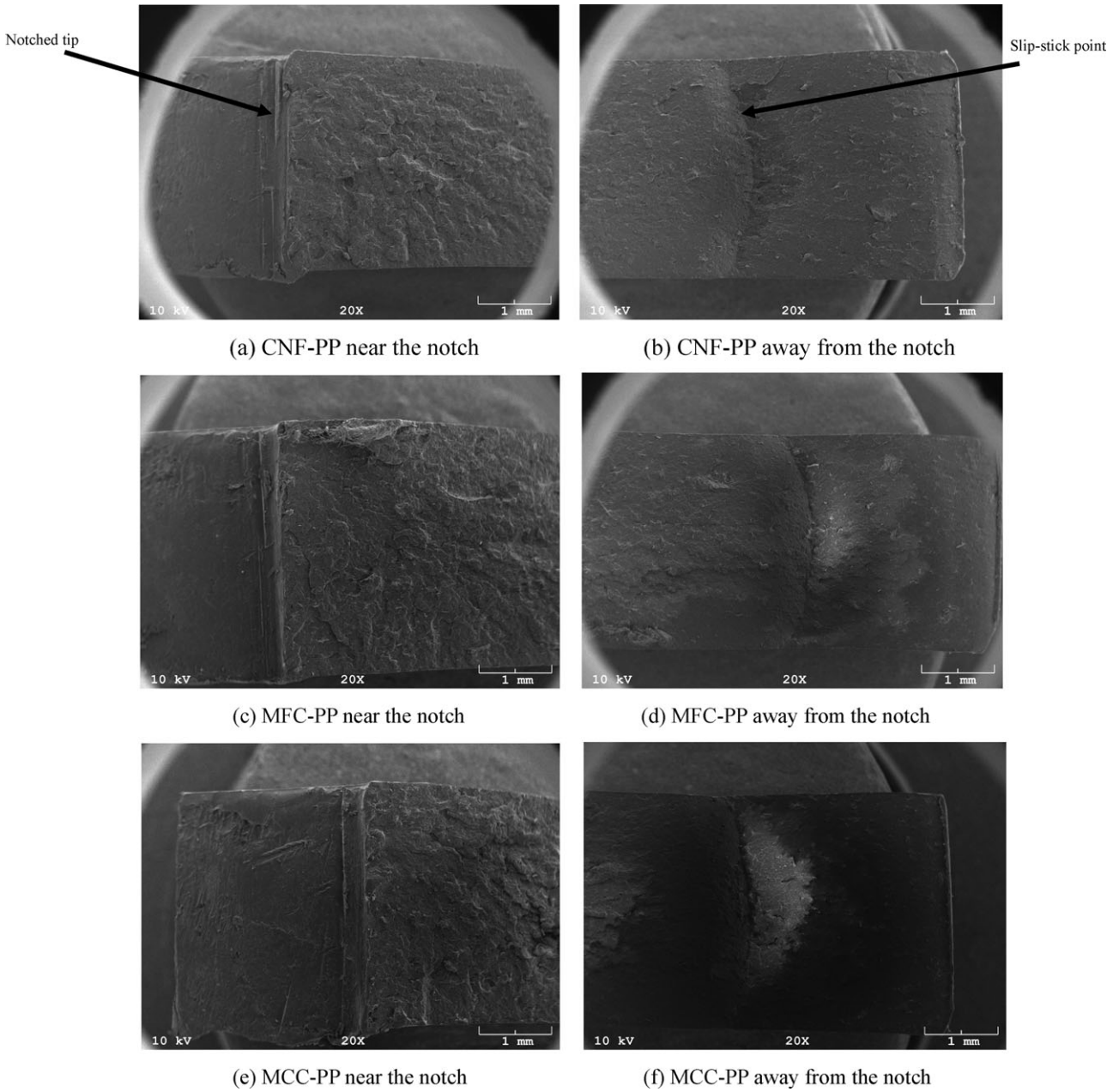

Figure 3. SEM micrographs of the composites notched impact samples at 20× magnification.

initiation zone. A stress whitened area which is the fracture initiation zone was taken into account as a fracture area (A). Work of fracture (W_f) means the energy consumed during the whole fracture process and consists of EWF (W_e) and work of propagation (W_p) as shown in Figure 2.

Work of fracture (W_f) means the energy consumed during the whole fracture process and consists of EWF (W_e) and work of propagation (W_p) as shown in eq. (1).

$$W_f = W_e + W_p \tag{1}$$

$$W_e = w_e A = w_e tl \tag{2}$$

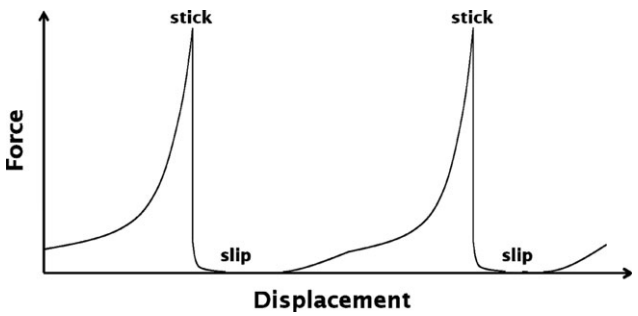

Figure 4. A schematic example of typical slip-stick force-displacement curve.

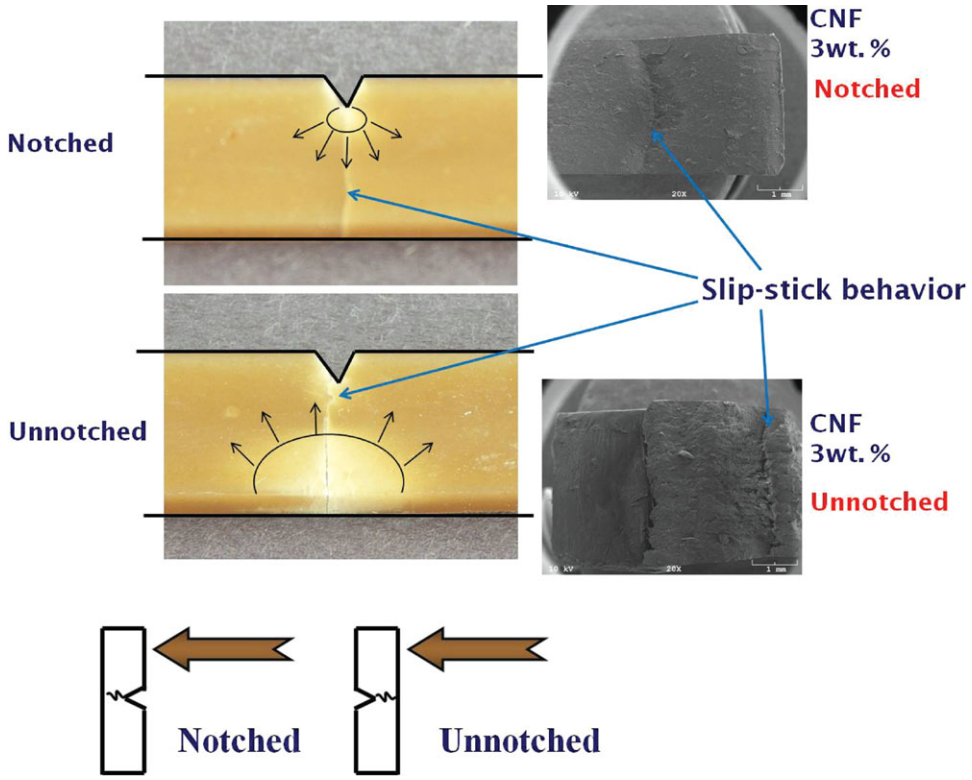

Figure 5. The slip-stick point in the notched and unnotched impact fracture samples. [Color figure can be viewed in the online issue, which is available at wileyonlinelibrary.com.]

$$W_p = \beta w_p A l = \beta w_p t l^2 \quad (3)$$

EWF (W_e) means the energy consumed to initiate fracture which is the specific EWF (w_e) multiplied by fracture area (A) as shown in eq. (2). Work of propagation (W_p) means the energy consumed to propagate fracture which is specific work of propagation (w_p) multiplied by shape parameter (β), fracture area (A), and ligament length (l) because it is related to the volume of fracture zone as shown in eq. (3). Specific work of fracture (w_f) is the work of fracture (W_f) divided by fracture area ($A = tl$, t: thickness). Multiple specific works of fracture (w_f) data points can be obtained at different ligament lengths (l) and a linear regression line can be obtained as shown in eq. (4). Specific work of fracture (w_f) can be simplified as a linear function as shown in eq. (5). Specific EWF (w_e) is the y intercept and specific work of propagation (w_p) multiplied by shape parameter (β) is the slope of the regression line. Shape parameter (β) is $\pi/4$ because the fracture zone is circular in this case[26] as shown in eq. (4). Finally, the specific EWF (w_e) and specific work of propagation (w_p) can be obtained and then the amount of energy consumed during fracture initiation [specific EWF (w_e)] and fracture propagation [specific work of propagation (w_p)] can be obtained as shown in eq. (6).

$$w_f = w_e + \beta w_p l, \quad \beta = \pi/4 \quad (4)$$

$$y = C + ax \quad (5)$$

$$w_e = C(kJ/m^2), \quad w_p = a/\beta(MJ/m^3) \quad (6)$$

RESULTS AND DISCUSSION

Morphological Characterization Using Scanning Electron Microscopy

The fracture surfaces of the 3 wt % CNF, MFC, and MCC-filled PP notched impact samples near the notch at 20× magnification are shown in Figure 3(a,c,e), respectively. The SEM micrographs clearly show the fracture surface at the notched tip which is a smooth and straight line at the stress concentrating point, which causes easy initiation and propagation of the crack when impact occurs.[17] This means that almost no energy was consumed to initiate impact fracture at the pre-generated stress concentrating point (notched tip). Figure 3(b,d,f) which show fracture surfaces of the composites notched impact samples away from the notch at 20× magnification, respectively. A slip-stick behavior is observed[18] in Figure 3(b,d,f). According to the impact strength analysis study,[19] it was found that the stress whitening occurred at the impact point as well as over the fracture initiation zone when the crack initiated and then propagated from the end of fracture initiation zone to slip-stick point.[18] Beyond the slip-stick point, there is no impact resistance and it is a brittle fracture zone. The smooth surface beyond the slip-stick point indicates that the crack propagated without resistance as shown in Figure 4 which means that the whole fracture surface consisted of the fracture initiation zone, fracture propagation zone, and brittle fracture zone. Usually slip-stick behavior (also known as stick-slip behavior) can be seen on PSA (pressure sensitive adhesives) tapes or plain surfaces which experience a frictional force (such as moving a table

Applied Polymer SCIENCE

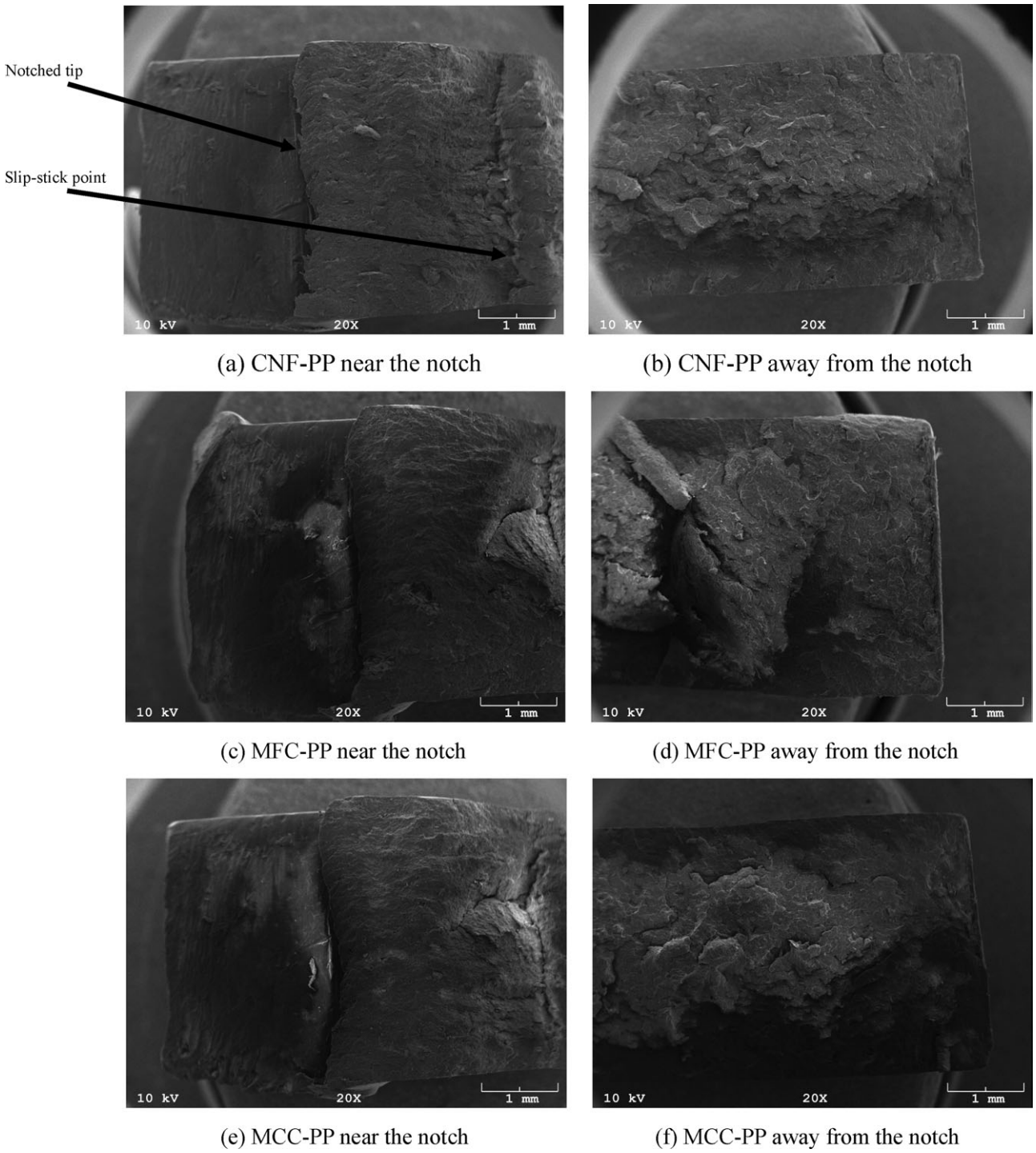

Figure 6. SEM micrographs of the composites unnotched impact samples at 20× magnification.

or chair across the floor). Once the strain sticks at a certain point, the frictional force will be accumulated and when the stress reaches the proportional limit, strain will extend suddenly with no frictional force for a while. Beyond the slip-stick point, there is no resistance or frictional force. A slip-stick behavior is observed in both of notched and unnotched impact samples as shown in Figure 5.

The fracture surfaces of the 3 wt % CNF, MFC, and MCC-filled PP unnotched impact samples near the notch at 20× magnification are shown in Figure 6(a,c,e), respectively. An irregularly fractured notched tip is observed and this indicates that the notched tip might not be a stress concentrating point, but can be attributed to the fractured interfacial area between the reinforcement and matrix polymer because the impact fracture

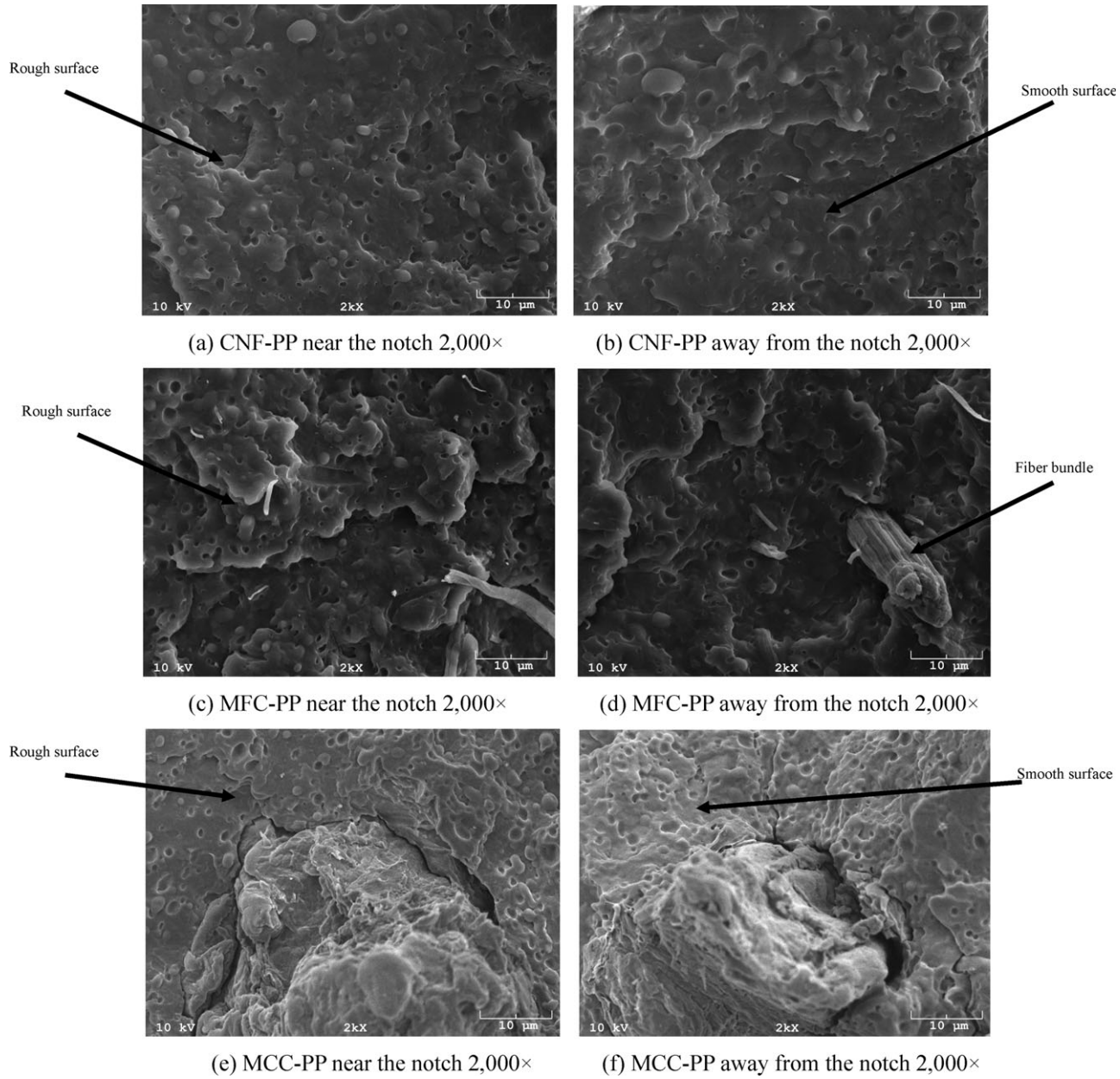

Figure 7. SEM micrographs of the composites notched impact samples at 2000×.

initiated from the opposite side and propagated to the notched tip. Slip-stick point was also observed. Figure 6(b,d,f) shows fracture surfaces of the composites unnotched impact samples away from the notch where the fracture initiated at 20× magnifications, respectively. The unnotched sample shows an uneven fracture surface, which is the fractured interfacial area between the reinforcement and matrix polymer.[17] Since this is a fracture initiated zone, a very rough fracture surface is observed.

The fracture surfaces of the 3 wt % CNF, MFC, and MCC-filled PP notched impact samples near and away from the notch at different magnifications are shown in Figures 7 and 8. A few short fibers, which are less than 250 nm in diameter are observed in Figure 8(a,b); a few MFC fiber bundles and individual fibrils less than 300 nm in diameter can be observed in Figures 7(d) and 8(c,d); MCC particles are observed larger than 10 μm size range in Figure 7(e,f), but with the main component being matrix polymer; Figure 8(e,f) show the reinforcement-matrix debondings at the interface between MCC and PP matrix which causes non-uniform stress transfer when the impact loading is applied. SEM micrographs of individual CNF, MFC, and MCC were shown together for comparison in previous study.[19] The fracture initiation zone near the notched tip in notched impact samples as shown in Figure 7(a,c,e) represent a rough fracture surface compared with the brittle propagation zone away from the notched tip in notched impact samples as shown in Figure 7(b,d,f) because the fracture initiated from the notched tip and propagated to the other side.

Applied Polymer SCIENCE

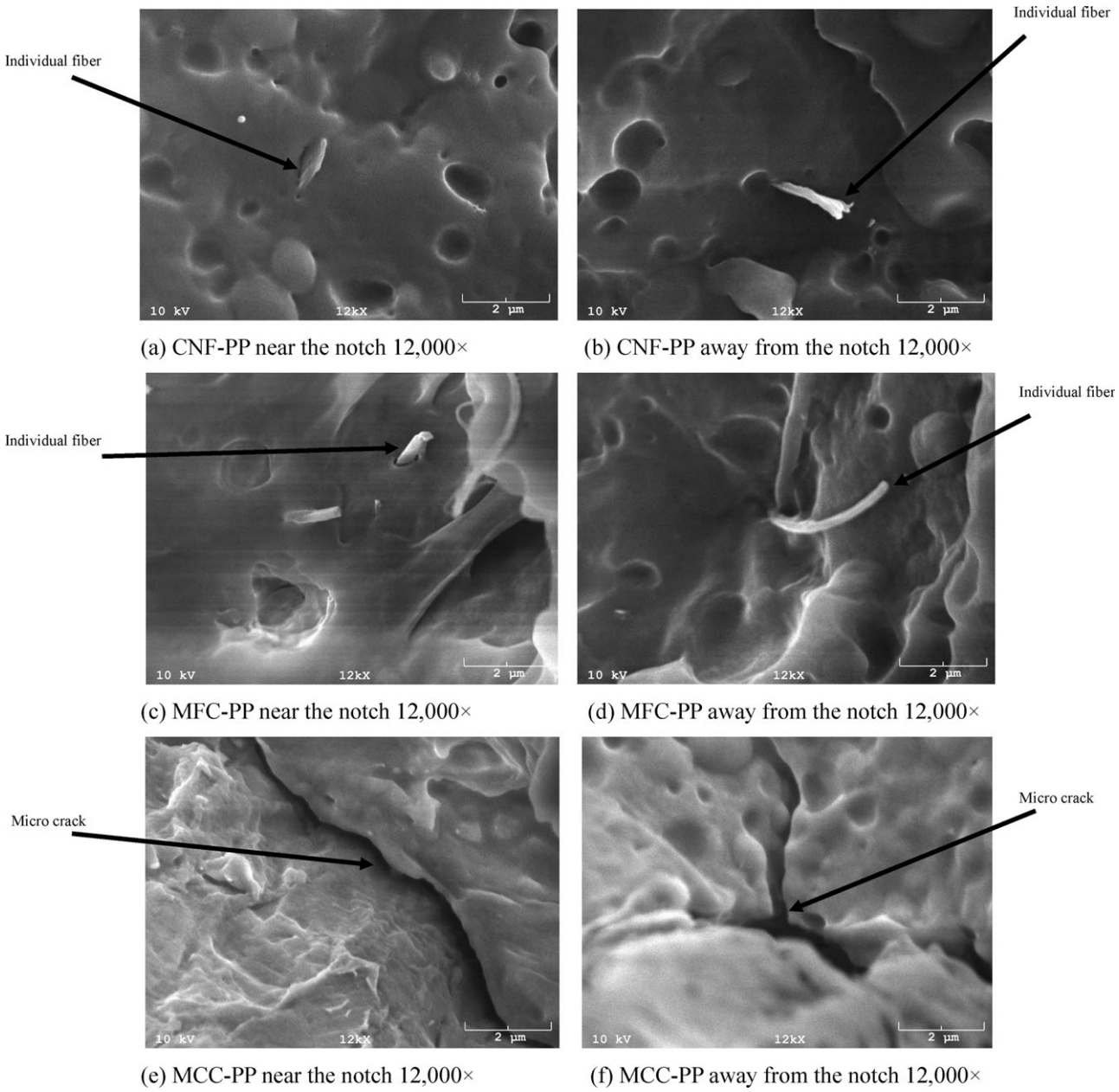

Figure 8. SEM micrographs of the composites notched impact samples at 12,000×.

The fracture surfaces of the 3 wt % CNF, MFC, and MCC-filled PP unnotched impact samples near and away from the notch where the fracture was initiated at different magnifications are shown in Figures 9 and 10. The fracture surfaces in Figure 9(a,c,e) appear to be smooth which is similar to notched fracture surfaces away from the notched tip because the crack initiated from the other side and only propagated to near the notch. On the other hand, a rough fracture surface can be observed since this is a fracture initiated zone as shown in the Figure 9(b,d,f) because of the crack initiated at the interface between the reinforcement and matrix polymer.[17] In the narrow range, surfaces are all appear to be rough. But if we consider overall altitude in the whole range of SEM pictures, Figure 9(b,d,f) indicate more up and down, hill and valley shape than Figure 9(a,c,e). In Figures 9(e) and 10 (e), there are reinforcement-matrix debondings between the MCC and PP matrix and this caused non-uniform stress transfer and decreased impact strength compared with the neat PP samples as indicated in an impact strength analysis study.[19] In Figures 9(f) and 10(f), more severe cracks can be observed because away from the notch is a fracture initiated region which means that cavitation and debonding occurred at the interface between the reinforcement and matrix polymer.[45]

Overall, the individual CNF fibers 50–300 nm in diameter and MFC fibrils 50–500 nm in diameter which are smaller than MCC particles 50 μm in average diameter have been observed from the SEM micrographs in the impact fracture surfaces. Generally, the individual MCC particles appear to be irregular

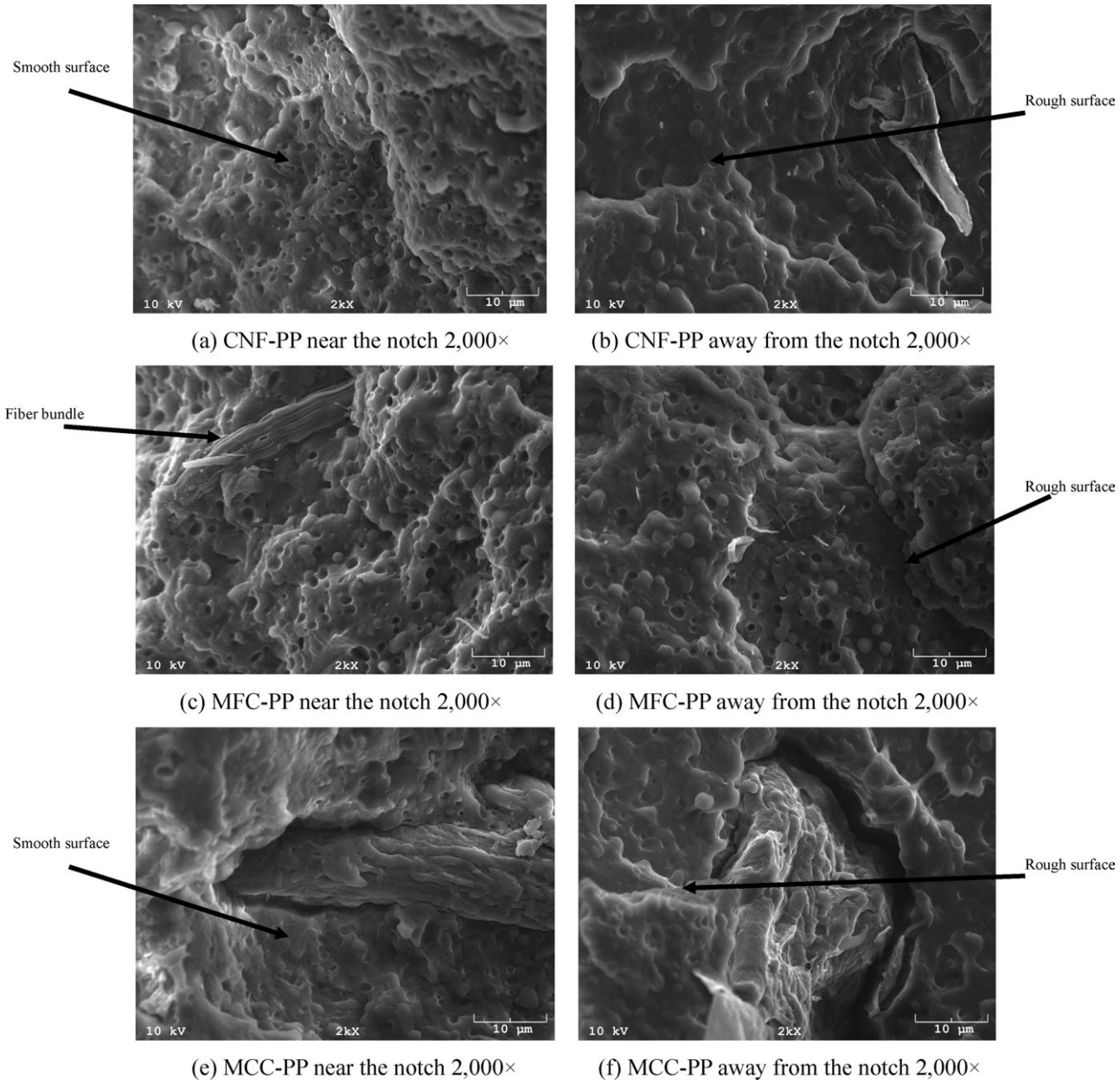

Figure 9. SEM micrographs of the composites unnotched impact samples at 2000×.

and larger than CNF and MFC in the SEM micrographs. This means that the larger size-smaller interfacial area combination leading to smaller energy dissipation at the interfacial area between reinforcement and matrix polymer during the impact fracture process. The reinforcement-matrix debondings nearby larger MCC particles cause easy crack propagation between the MCC and matrix polymer during impact fracture and also contribute smaller energy dissipation at the interfacial area.

Essential Work of Fracture Analysis of Izod Impact Test Results

Specific EWF (w_e) values of CNF-filled PP composites notched impact tests were higher than those of MFC and MCC-filled PP composites as shown in Table I. CNF was the most excellent material among the others because the size of CNF is smallest and the shape is short rod-like form leading to a largest interfacial area which means that more energy is required to initiate fracture when impact loading is applied. In particular, CNF and MFC-filled composites look like without sacrificing its resistance with addition of reinforcement to the neat PP, meanwhile MCC-filled PP composites exhibit the lowest specific EWF (w_e) values because the largest particle size and smaller interfacial area leading to smaller energy dissipation at the interfacial area and also the reinforcement-matrix debondings nearby larger MCC particles cause easy crack propagation and contributes smaller energy dissipation at the interfacial area during the fracture process which is evidenced from the SEM investigations. The larger impact strength can be referenced to lower diameter

Applied Polymer SCIENCE

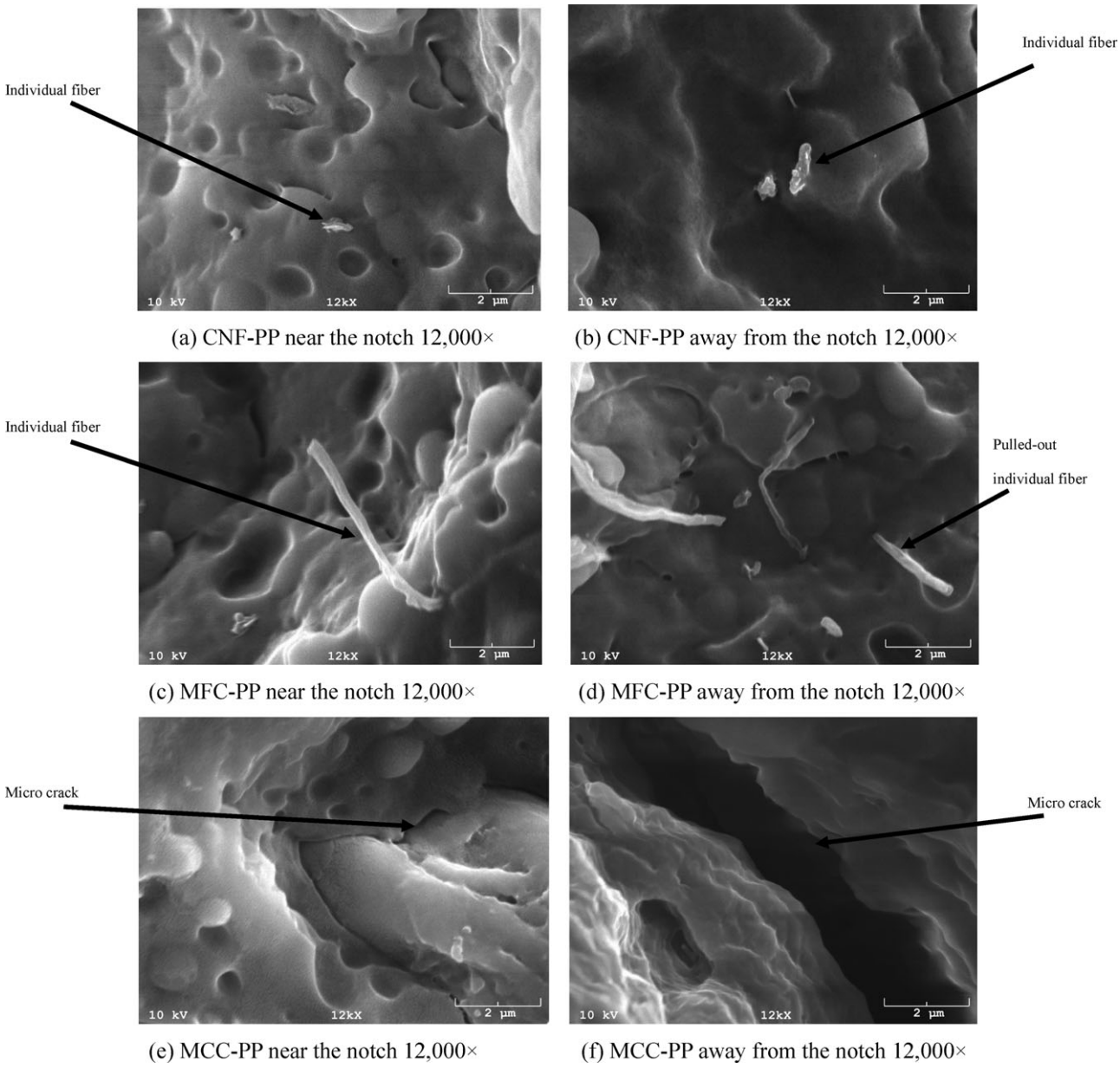

Figure 10. SEM micrographs of the composites unnotched impact samples at 12,000×.

of reinforcement material. It affects the filler/matrix interaction, whereby pull-outs appear more often with CNF and MFC than with MCC. It is supposed that for this reason the overall path length of initiated crack in CNF/MFC filled composites is being enlarged compared with MCC filled composites which results the large energy amount needed to break the sample.[46] In filled polymer composite system, the toughening is typically explained by invoking the two major deformation mechanisms of crazing and shear yielding of reinforcement material, but cavitation and particle deformation also play an important role.[47] Reinforcement pull-out is also important toughening mechanism[46] as shown in Figure 11[46–47] and it is the major toughening mechanism of the CNF and MFC filled composites in this study.

Table I. Specific Essential Work of Fracture (w_e) Values of the Composites by Notched Impact Test

	Specific essential work of fracture (KJ/m^2)		
Filler loading (wt %)	CNF	MFC	MCC
Neat PP	38.9	38.9	38.9
1	41.8	28.1	12.1
2	38.3	26.3	19.8
3	45.0	42.8	15.6
4	39.1	32.6	15.5
8	33.3	30.2	18.1

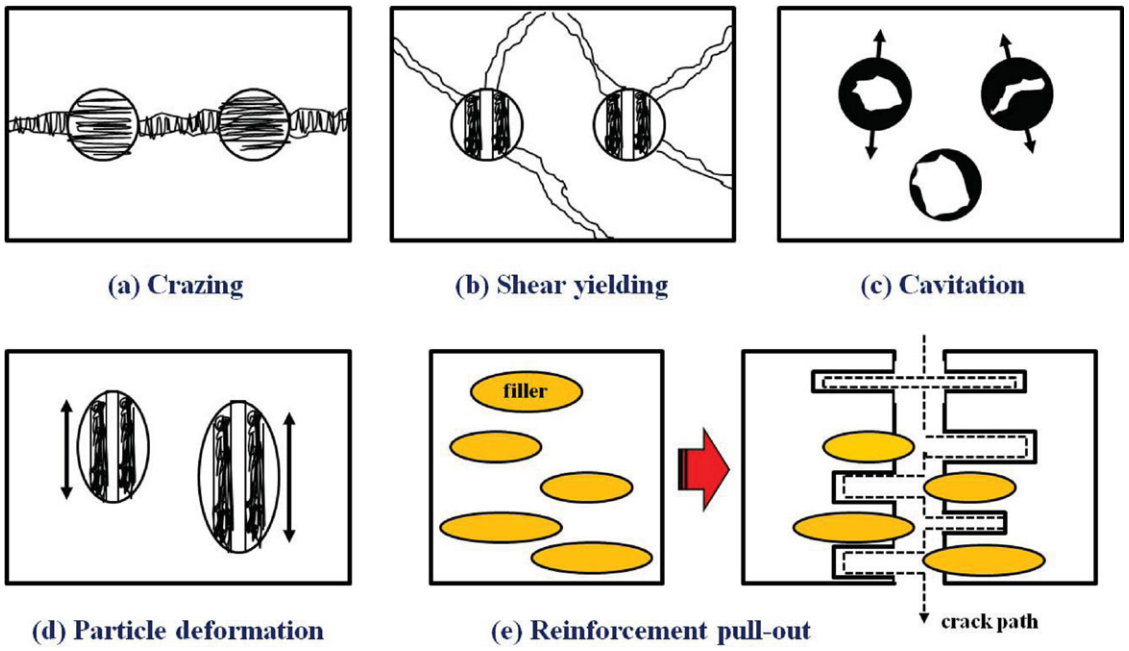

Figure 11. A schematic of five different toughening mechanisms.[46,47] [Color figure can be viewed in the online issue, which is available at wileyonlinelibrary.com.]

The neat PP, CNF, and MFC composite samples present no specific work of propagation (w_p) values as shown in Table II which means that the fracture propagates easily once the impact fracture is initiated. On the other hand, MCC filled PP composites present some resistance against the fracture propagation while those samples present very low resistance during the fracture initiation as shown in Table I which means that the larger particle size of MCC than CNF and MFC leading to the non-uniformity of reinforcement distribution in the matrix polymer as well as the fracture initiation-propagation energy combination. In other words, the fracture process usually consists of very hard initiation and easy propagation but easy initiation and hard propagation in the case of MCC-filled PP composite samples. Generally, the fracture was hard to initiate but easy to propagate in the composite materials used in this study which is consistent with the unique characteristics of the material and

Table II. Specific Work of Propagation (w_p) Values of the Composites by Notched Impact Test

	Specific work of propagation (MJ/m^3)		
Filler loading (wt %)	CNF	MFC	MCC
Neat PP	NR	NR	NR
1	NR	NR	5.1
2	NR	NR	1.8
3	NR	NR	2.7
4	NR	NR	4.0
8	NR	NR	0.3

NR: No resistance, β (shape factor) = $\pi/4$.

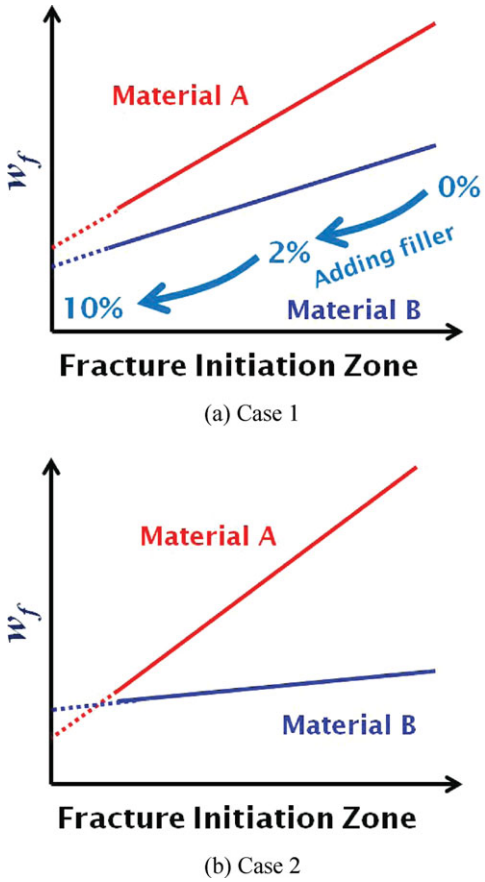

Figure 12. Case study of two different materials using EWF model. [Color figure can be viewed in the online issue, which is available at wileyonlinelibrary.com.]

is in good agreement with the analysis result in an impact strength analysis study.[19]

There are two possible scenarios comparing two different materials in terms of specific EWF and specific work of propagation as shown in Figure 12. In Case 1, both specific EWF and specific work of propagation values of Material A are higher than Material B, therefore Material A is recommended. Meanwhile in Case 2, specific EWF value of Material A is lower than Material B, but in terms of specific work of propagation value, Material A is higher than Material B. This means that fracture initiated relatively easily but once fracture is initiated, Material A is more resistant than Material B against fracture propagation. It is hard to initiate fracture in Material B but once fracture occurs, it is less resistant against fracture propagation. Considering all the possible end user applications, it is important for structural designers or material manufacturers to understand the practical implications of impact behavior depending on the specific applications, and also, to determine proper materials to be utilized.

CONCLUSIONS

1. This study presented SEM microscopy analysis of Izod impact fracture surfaces. In an impact strength analysis study,[19] the unnotched Izod impact energies were considerably larger than the notched Izod impact energies, and this was attributed to the different fracture processes involved in the notched and unnotched Izod impact samples. The SEM micrographs of the impact fracture surfaces of the composites help to explain different fracture processes involved in the notched and unnotched Izod impact tests. The fracture initiation zone represents rough fracture surface while the fracture propagation zone and brittle propagation zone represent smooth surfaces because the fracture initiated at the interface between reinforcement and matrix polymer and propagated along with the fracture propagation.
2. From the SEM investigation, CNF fibers and MFC fibrils are smaller than MCC particles even if the shape and aspect ratio are different which means that CNF and MFC fillers generate larger interfacial area than MCC-filled composites. Larger interfacial area leads larger energy dissipation. The reinforcement-matrix debondings nearby MCC particles cause easy crack propagation which contributes smaller energy dissipation than CNF and MFC-filled composites in the interfacial area. CNF is the best one based on the EWF analysis result that the EWF values obtained in the case of CNF-filled composites are higher than others.
3. The EWF concept is usable to analyze Izod impact test results because the EWF and specific work of propagation combination looks in agreement with impact resistance results and presents the same fracture behavior as the impact strength analysis study.[19] The visual inspection of the samples in which fracture was restrained indicates that crack propagated before complete ligament yielding which means that the yielding criterion is not satisfied. Despite the inconvenience in yielding criterion, EWF methodology is successfully employed in the composites used in this study.
4. As compared with the EWF values, work of propagation values is very low. This result indicates that the composite material is hard to initiate but easy to propagate the fracture. The trend of EWF is similar to that of standard notched Izod impact test. EWF concept by using Izod impact results is useful to structural designers or material manufacturers to consider end user applications and also will be helpful to determine proper materials to be utilized.

ACKNOWLEDGMENT

Funding for this research was provided by the National Science Foundation under Grant No. EPS-05-54545 and the US Army W912HZ-07-2-0013.

REFERENCES

1. Mi, Y.; Chen, X.; Guo, Q. *J. Appl. Polym. Sci.* **1997,** *64*, 1267.
2. Alemdar, A.; Sain, M. *Compos. Sci. Technol.* **2008,** *68*, 557.
3. Marcovich, N. E; Auad, M. L.; Bellesi, N. E.; Nutt, S. R.; Aranguren, M. I. *J. Mater. Res.* **2006,** *21*, 870.
4. Eichhorn, S. J.; Young, R. J. *Cellulose.* **2001,** *8*, 197.
5. Goussé, C.; Chanzy, H.; Cerrada, M. L.; Fleury, E. *Polymer* **2004,** *45*, 1569.
6. Hubbe, M.A; Rojas, O.J; Lucia, L.A; Sain, M. *Bioresources.* **2008,** *3*, 929.
7. Abe, K.; Iwamoto, S.; Yano, H. *Biomacromolecules* **2007,** *8*, 3276.
8. Cheng, Q.; Wang, S. Q.; Rials, T. G.; Lee, S. H. *Cellulose* **2007,** *14*, 593.
9. Dalmas, F.; Chazeau, L.; Gauthier, C.; Cavaille, J. Y.; Dendievel, R. *Polymer* **2006,** *47*, 2802.
10. Dufresne, A.; Dupeyre, D.; Vignon, M. R. *J. Appl. Polym. Sci.* **2000,** *76*, 2080.
11. Wu, Q.; Henriksson, M.; Liu, X.; Berglund, L. A. *Biomacromolecules* **2007,** *8*, 3687.
12. Bengtsson, M.; Baillif, M. L.; Oksman, K. *Compos. Part A-Appl. Surf.* **2007,** *38*, 1922.
13. Svoboda, P.; Zeng, C.; Wang, H.; Lee, L. J.; Tomasko, D. L. *J. Appl. Polym. Sci.* **2002,** *85*, 1562.
14. Hristov, V. N.; Lach, R.; Grellmann, W. *Polym. Test* **2004,** *23*, 581.
15. Oksman, K.; Clemons, C. *J. Appl. Polym. Sci.* **1998,** *67*, 1503.
16. Stark, N. M.; Rowlands, R. E. *Wood Fiber. Sci.* **2003,** *35*, 167.
17. Yang, H. S.; Kim, H. J.; Son, J.; Park, H. J.; Lee, B. J.; Hwang, T. S. *Compos. Struct.* **2004,** *63*, 305.
18. Yuan, Q.; Misra, R. D. K. *Polymer* **2006,** *47*, 4421.
19. Yang, H. S.; Gardner, D. J.; Nader, J. W. *Compos. Part A-Appl. Surf.* **2011,** *42*, 2028.

20. Kvien, I.; Tanem, B. S.; Oksman, K. *Biomacromolecules* **2005,** *6*, 3160.
21. Ahmad, S. H.; Rasid, R.; Surip, S. N.; Anuar, H.; Czigany, T.; Abdul Razak, S. B. *J. Compos. Mater.* **2007,** *41*, 2147.
22. Arencón, D.; Velasco, J. I.; Realinho, V.; Antunes, M.; Maspoch, M. L. *Polym. Test.* **2007,** *26*, 761.
23. Bureau, M. N.; Perrin-Sarazin, F.; Ton-That, M. *Polym. Eng. Sci.* **2004,** *44*, 1142.
24. Bureau, M. N.; Ton-That, M.; Perrin-Sarazin, F. *Eng. Fract. Mech.* **2006,** *73*, 2360.
25. Gong, G.; Xie, B.; Yang, W.; Li, Z.; Zhang, W.; Yang, M. *Polym. Test.* **2005,** *24*, 410.
26. Martinez, A. B.; Gamez-Perez, J.; Sanchez-Soto, M.; Velascom, J. I.; Santana, O. O.; Maspoch, M. L. *Eng. Fail. Anal.* **2009,** *16*, 2604.
27. Qiao, Y.; Avlar, S.; Chakravarthula, S. S. *J. Appl. Polym. Sci.* **2005,** *95*, 815.
28. Saminathan, K.; Selvakumar, P.; Bhatnagar, N. *Polym. Test.* **2008a,** *27*, 296.
29. Saminathan, K.; Selvakumar, P.; Bhatnagar, N. *Polym. Test.* **2008b,** *27*, 453.
30. Gray, A. Testing Protocol for Essential Work of Fracture; *European Structural Integrity Society* (ESIS), **1993** – TC4.
31. Yu, H.; Zhang, Y.; Ren, W. *J. Appl. Polym. Sci.* **2009,** *113*, 181.
32. Gonzalez, I.; Eguiazabal, J. I.; Nazabal, J. *Polym. Test.* **2009,** *28*, 760.
33. Ozkoc, G.; Bayram, G.; Bayramli, E. *J. Mater. Sci.* **2008,** *43*, 2642.
34. Wainstein, J; Fasce, L.A; Cassanelli, A; Frontini, P.M. *Eng. Fract. Mech.* **2007,** *74*, 2070.
35. Yoo, Y.; Shah, R. K.; Paul, D. R. *Polymer* **2007,** *48*, 4867.
36. Bao, S. P.; Tjong, S. C. *Compos. Part A-Appl. Surf.* **2007,** *38*, 378.
37. Tjong, S. C.; Bao, S. P. *J. Polym. Sci. Polym. Phys.* **2005,** *43*, 585.
38. Pettarin, V.; Frontini, P. M.; Elicabe, G. E. *Polym. Test.* **2005,** *24*, 189.
39. Tjong, S. C.; Xu, S. A.; Mai, Y. W. *Mater. Sci. Eng. A-Struct.* **2003,** *347*, 338.
40. Ching, E. C. Y.; Li, R. K. Y.; Tjong, S. C.; Mai, Y. W. *Polym. Eng. Sci.* **2003,** *43*, 558.
41. Fasce, L.; Bernal, C.; Frontini, P.; Mai, Y. W. *Polym. Eng. Sci.* **2001,** *41*, 1.
42. Lach, R.; Schneider, K.; Weidisch, R.; Janke, A.; Knoll, K. *Eur. Polym. J.* **2005,** *41*, 383.
43. Vu-Khanh, T.; de Charentenay, F. X. *Polym. Eng. Sci.* **1985,** *25*, 841.
44. Kudva, R. A.; Keskkula, H.; Paul, D. R. *Polymer* **2000,** *41*, 335.
45. Zhang, Q. X.; Yu, Z. Z.; Xie, X. L.; Mai, Y. W. *Polymer* **2004,** *45*, 5985.
46. Bledzki, A. K.; Jaszkiewicz, A.; Scherzer, D. *Compos. Part A-Appl. Surf.* **2009,** *40*, 404.
47. Jain, A. K.; Nagpal, A. K.; Singhal, R.; Gupta, N. K. *J. Appl. Polym. Sci.* **2000,** *78*, 2089.